Journal Pre-proofs

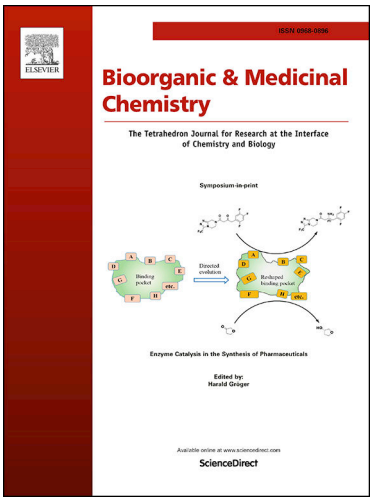

Synthesis and Biological Activity of Thieno[3,2-*d*]pyrimidines as Potent JAK3 Inhibitors for the Treatment of Idiopathic Pulmonary Fibrosis

Yanming Zhu, Xu Zheng, Changyuan Wang, Xiuli Sun, Huijun Sun, Tengyue Ma, Yanxia Li, Kexin Liu, Lixue Chen, Xiaodong Ma

PII: S0968-0896(19)31714-6
DOI: https://doi.org/10.1016/j.bmc.2019.115254
Reference: BMC 115254

To appear in: *Bioorganic & Medicinal Chemistry*

Received Date: 6 October 2019
Revised Date: 5 December 2019
Accepted Date: 6 December 2019

Please cite this article as: Y. Zhu, X. Zheng, C. Wang, X. Sun, H. Sun, T. Ma, Y. Li, K. Liu, L. Chen, X. Ma, Synthesis and Biological Activity of Thieno[3,2-*d*]pyrimidines as Potent JAK3 Inhibitors for the Treatment of Idiopathic Pulmonary Fibrosis, *Bioorganic & Medicinal Chemistry* (2019), doi: https://doi.org/10.1016/j.bmc.2019.115254

Synthesis and Biological Activity of Thieno[3,2-*d*]pyrimidines as Potent JAK3 Inhibitors for the Treatment of Idiopathic Pulmonary Fibrosis

Yanming Zhu[a,1], Xu Zheng[a,1], Changyuan Wang[a], Xiuli Sun[b], Huijun Sun[a], Tengyue Ma[c], Yanxia Li[b], Kexin Liu[a], Lixue Chen[a,*] and Xiaodong Ma[a,*]

[a] *College of Pharmacy, College of Basic Medical Science, Dalian Medical University, Dalian 116044, PR China.*

[b] *Department of Hematology, Institute of Respiratory Diseases, the First Affiliated Hospital of Dalian Medical University, Dalian 116011, PR China.*

[c] *Dalian Buyun Biological Technology Co., Ltd., 116085, PR China.*

[1] *These authors contributed equally to this work.*

E-mail address: chenlx2016@126.com

Abstract

Idiopathic pulmonary fibrosis (IPF) is a serious and fatal lung disease, with a median survival of only 3 to 5 years from diagnosis. Janus kinase 3 (JAK3) has a well-established role in the pathogenesis of various autoimmune diseases, including rheumatoid arthritis (RA) and autoimmune-related pulmonary fibrosis. In this study, through the use of a conformationally-constrained design strategy, a series of thieno[3,2-*d*]pyrimidines were synthesized as potent JAK3 inhibitors for the treatment of IPF. Among them, the most potent JAK3 inhibitor, namely **8e** (IC_{50}=1.38 nM), significantly reduced the degree of airsacculitis and fibrosis according to hematoxylin-eosin (HE) staining assay for the lung tissue in the bleomycin (BLM)-induced pulmonary fibrosis mouse model. The clear reduction of the lung collagen deposition by the determination of Masson and hydroxyproline (HYP) content also demonstrated its efficacy in the treatment of fibrosis. In addition, **8e** also reduced the expression of the inflammatory markers IL-6, IL-17A, TNF-α and malondialdehyde (MDA) in lung tissue, which indicated its higher anti-inflammatory activity compared with that of the reference agents (nintedanib and gefitinib). Furthermore, it possessed low cytotoxicity against normal human bronchial epithelia (HBE) cells (IC_{50}>39.0 μM) and C57BL mice.

All these evaluated biological properties suggest that **8e** may be a potential JAK3 inhibitor for the treatment of IPF.

Key words: Idiopathic pulmonary fibrosis; JAK inhibitors; thieno[3,2-*d*]pyrimidines

1. Introduction

Idiopathic pulmonary fibrosis (IPF) is a fatal lung disease, with a median survival between 3 and 5 years from diagnosis, characterized by alveolar epithelial injury and hyperplasia, inflammatory cell accumulation, fibroblast proliferation, and deposition of extracellular matrix with fibrotic lesions [1–3]. The annual incidence of IPF in the U.S. has been estimated to be between 6.8−8.8 cases per 100,000 population using narrow case definitions and between 16.3−17.4 per 100,000 population using broad case definitions. Recent analysis of IPF-related mortality data from the U.S. indicates that the age-adjusted mortality rate has increased to 28.4% in men and 41.3% in women [4]. Even more serious is that the incidence of IPF continues to increase every year. Accordingly, although IPF is not cancer, it causes more harm than cancer.

Currently, there are only two drugs approved by the U.S. Food and Drug Administration (FDA) for the treatment of IPF, namely pirfenidone (**1**, Esbriet) and nintedanib (**2**, Ofev). Pirfenidone is an orally available pyridone derivative that has been approved for the treatment of IPF in various countries, including Japan, India, China, Europe, Canada, and the United States [5]. Although the precise mode of action of pirfenidone has not yet been established, its antifibrotic, anti-inflammatory, and antioxidant properties have been demonstrated [6, 7]. The antifibrotic properties of pirfenidone are attributed to its ability to reduce the expression of cytokines, such as TGF-β, leading ultimately to inhibition of fibrosis [8]. Nintedanib [9], formerly known as BIBF1120, is an indolinone derivative

that was identified through a lead compound optimization strategy designed for angiogenesis inhibitors with anticancer effects. Nintedanib is a potent, orally available, triple tyrosine kinase inhibitor that targets the PDGF receptors α/β, FGF receptors, and all three vascular endothelial growth factor (VEGF) receptor subtypes [10, 11]. Pirfenidone and nintedanib significantly reduce the rate of disease progression. However, these two drugs do not stop or reverse the deterioration of IPF and thus have shown no benefit in the overall survival of patients with IPF.

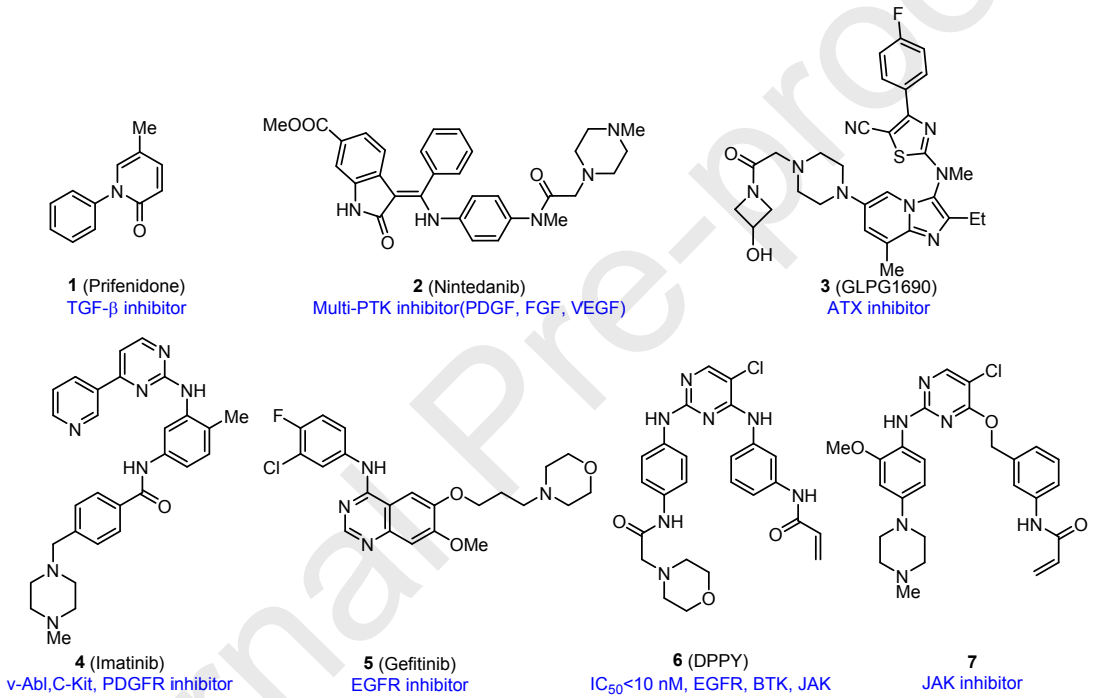

Fig. 1. Chemical structures of the typical anti-IPF agents and JAK3 inhibitors.

Tyrosine kinases are known to regulate various signaling pathways involved in maintaining cellular homeostasis, including the pathogenesis of pulmonary fibrosis [12–14]. For instance, the novel anti-IPF agent nintedanib blocks VEGFR1, VEGFR2, VEGFR3, FGFR1, FGFR2, FGFR3, PDGFRα, and PDGFRβ and etc.. The novel autotaxin inhibitor GLPG1690 (**3**) [15] showed great efficacy in a bleomycin (BLM)-induced pulmonary fibrosis model in mice and in reducing extracellular matrix deposition in the lung. GLPG1690 is currently being evaluated in an exploratory

phase III study in patients with idiopathic pulmonary fibrosis (ClinicalTrials.gov; Identifier: NCT03733444). Imatinib (**4**) [16] is a multi-target inhibitor of v-Abl, c-Kit and PDGFR, which also has been shown to have potential efficacy in the treatment of fibrotic lung disease (ClinicalTrials.gov; Identifier: NCT00131274). Gefitinib (**5**) [17], a typical EGFR inhibitor that was approved in 2003 by the U.S. FDA for the treatment of non-small cell lung cancer (NSCLC), has also been found to have a significant protective effect on BLM-induced lung fibrosis *via* EGF. (**Fig. 1**)

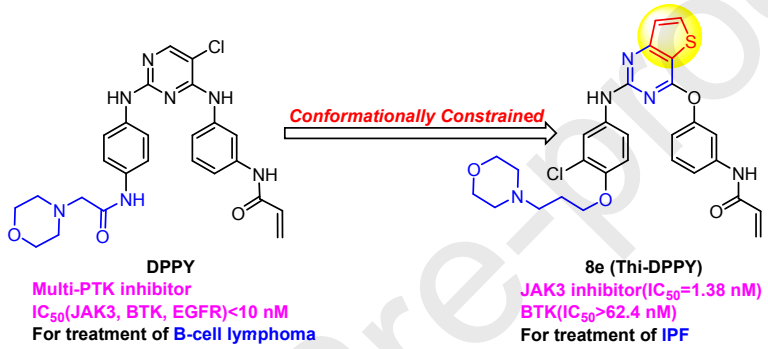

Fig. 2. Design of conformation-constrained Thi-DPPY derivative as JAK3 inhibtor.

Janus kinases (JAKs) are a family of cytoplasmatic tyrosine kinases which due to their roles in cytokine signaling processes are attractive targets for the development of anti-inflammatory drugs [18, 19]. Given that JAK3 functions are restricted to immune cells, an isoform-selective inhibitor for JAK3 could be particularly useful to achieve more clinically effective and precise effects [20, 21]. In our previous study, we identified a family of diphenylpyrimidines (DPPYs) as potent JAK3 and BTK dual inhibitors, and most of them exhibited strong anti-proliferative activity against B-cell lymphoma cells [22]. However, most of these DPPYs also could blocked BTK activity, and had low selectivity for JAK3. In this study, a series of thieno[3,2-*d*] diphenylpyrimidines (Thi-DPPYs) were designed through a conformationally-constrained design strategy, and many of them not only showed improved selectivity for JAK3, but also enhanced activity against IPF *in vivo* (**Fig. 2**). The synthesis and

evaluation of their biological activity were described in this study.

2. Results and discussion

2.1 Chemistry

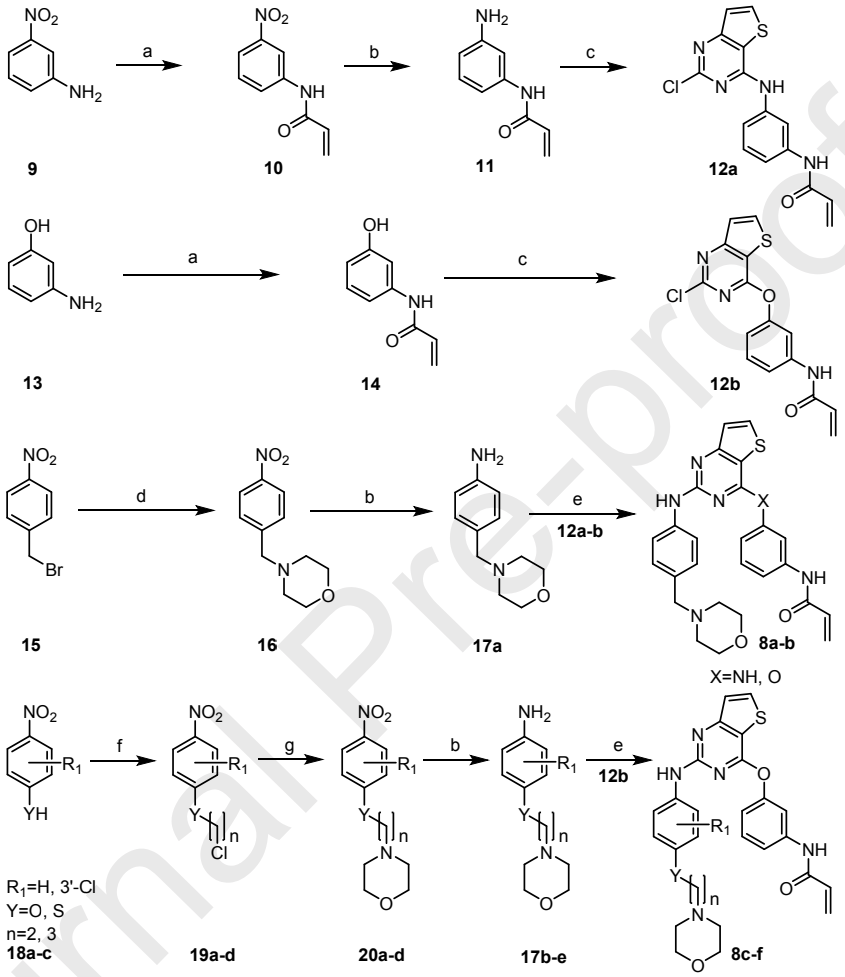

Scheme 1. The synthetic route of target compounds **8a-f**.

Reagents and conditions: a) Acryloylchloride, $NaHCO_3$, CH_3CN, 0 °C, 0.5 h, 81–92%; b) Fe-aq. NH_4Cl, MeOH–H_2O, 70 °C, 2 h, 71–85%; c) 2,4-dichlorothiopheno [3,2-*d*]pyrimidine, DIPEA, 1, 4-dioxane, 80 °C, 5 h, 35–71%; d) Morpholine, K_2CO_3, DMF, rt, 5 h, 95%; e) *p*-Toluenesulfonic acid, *n*-BuOH, 70 °C, 6 h, 45–60%; f) 1-bromo-2-chloroethane/1-bromo-3-chloropropane, K_2CO_3, CH_3CN, 40 °C, 6 h, 77–82%; g) Morpholine, K_2CO_3, KI, CH_3CN, 80 °C, 5 h, 81–88%.

All the Thi-DPPYs were synthesized as illustrated in **Scheme 1**, according to our previously reported methods [23]. The commercially available starting material 3-nitroaniline (**9**) was reacted with acryloyl chloride to give **10** which was reduced in the presence of Fe-aq. NH_4Cl to produce intermediate **11**. Then the substitution of the *C*-4 chloride atom in 2,4-dichlorothiopheno[3,2-

d]pyrimidine with **11** to produce the key intermediate **12a**. **12b** was obtained by application of the similar synthetic route. For the synthesis of **16**, bromine atom in 4-nitrobenzyl bromide was conveniently substituted with morpholine, then reduced the nitro group to an amino group. Additionally, **18a-c** was reacted with 1-bromo-2-chloroethyane or 1-bromo-3-chloropropane to synthesize **19a-d**. Intermediate **19a-d** was reacted with morpholine and then **17b-e** was prepared *via* reduction reaction. The nucleophilic substitution reaction of the helium atom in **12a-b** with **17a-e** was carried out under the action of *p*-toluenesulfonic acid (*p*-TsOH) to generate the desired **8a-f**.

2.2 Biological activity

2.2.1 Enzymatic activity and toxicity in vitro

All the title molecules were evaluated for their activity against BTK and JAK3 kinases using the ADP-Glo^{TM} assay kit (Promega, Madison, WI, USA). The kinase inhibitory activity results, shown in **Table 1**, indicated that most of these title compounds strongly inhibited the JAK3 enzymatic activity at concentrations in the range of 1.38 to 90.8 nM. Among them, compound **8e** not only exhibited the strongest anti-JAK3 activity (IC_{50}=1.38 nM), but also strongly interfered with the activity of BTK (IC_{50}=62.4 nM). However, the other compounds seem to be less potent against BTK kinase at concentrations lower than 100 nM. These kinase-based test result revealed that the chloro-substituent at the *C*-3 position of the aniline ring is useful to enhance the anti-kinase activity. In addition, all these compounds were also evaluated for their cytotoxicity against the normal human bronchial epithelial (HBE) cells. The evaluation results revealed that these compounds have low cell toxicity (IC_{50}>8.27 μM). Overall, this study identified a potent JAK3 inhibitor, namely **8e**, whose biological activity as potential application for the treatment of IPF warrant further investigation.

Table 1. *In vitro* enzymatic activity and toxicity to HBE cells of the title compounds **8a-f** [a].

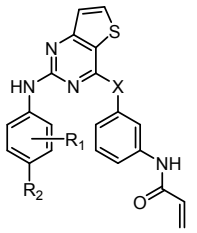

Compd.	X	R_1	R_2	Enzymatic activity (IC_{50}, nM) [b]		Toxicity to HBE cells (IC_{50}, μM) [c]
				BTK	JAK3	HBE cells
8a	NH	H		>100	59.39	8.27
8b	O	H		>100	85.3	12.8
8c	O	H	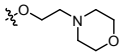	>100	90.8	23.3
8d	O	H	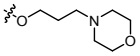	>100	89.2	>40.0
8e	O	3'-Cl	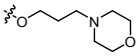	62.4	1.38	39.0
8f	O	H	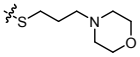	>100	46.0	>40.0
HM71224					14.6	
spebrutinib					66.5	
ibrutinib					16.1	

[a] The data were means of three separate experiments. [b] The enzymatic activity against BTK and JAK3 enzymes using the ADP-Glo™ kinase assay. [c] The toxicity effects on the proliferation of HBE cells was determined by the CCK-8 assay.

2.2.2 ***8e*** *attenuated the pulmonary morphology changes induced by BLM in mouse lung*

The therapeutic effect of **8e** was investigated *in vivo* using the BLM-induced pulmonary inflammation and pulmonary fibrosis model in C57BL mice. For comparison, novel agents for treatment of IPF, including the multi-protein tyrosine kinase inhibitor nintedanib, the EGFR inhibitor gefitinib, and pifenidone were evaluated as well. As shown in **Fig. 3a** and **3b**, after administration of **8e** at a dose of 30 or 60 mg/kg for 14 days, the structural confusion of the lung tissue and obvious swelling in the alveolar septum observed by HE staining was clearly improved, achieving similar therapeutic effects as nintedanib at a dose of 60 mg/kg. Notably, the therapeutic effect of **8e** at a

dosage of 60 mg/kg was significantly better than those of the pifenidone (120 mg/kg), gefitinib (60 mg/kg) groups. Additionally, the therapeutic effect of **8e** at 60 mg/kg was significantly better than that at 30 mg/kg, indicating that its effect was dose-dependent. In general, the higher of the lung coefficient reflected the worse of the therapeutic effect [24]. Evidently, **8e** significantly reduced the lung coefficient in the mice of the BLM-induced pulmonary fibrosis model group (**Fig. 3c**), revealing its enhanced anti-IPF efficacy. Taken together, these results indicated that the therapeutic effect of **8e** is similar to that exerted by the same dose of nintedanib, and superior to those of the high dosage (120 mg/kg) of pifenidone and the dose of gefitinib (60 mg/kg).

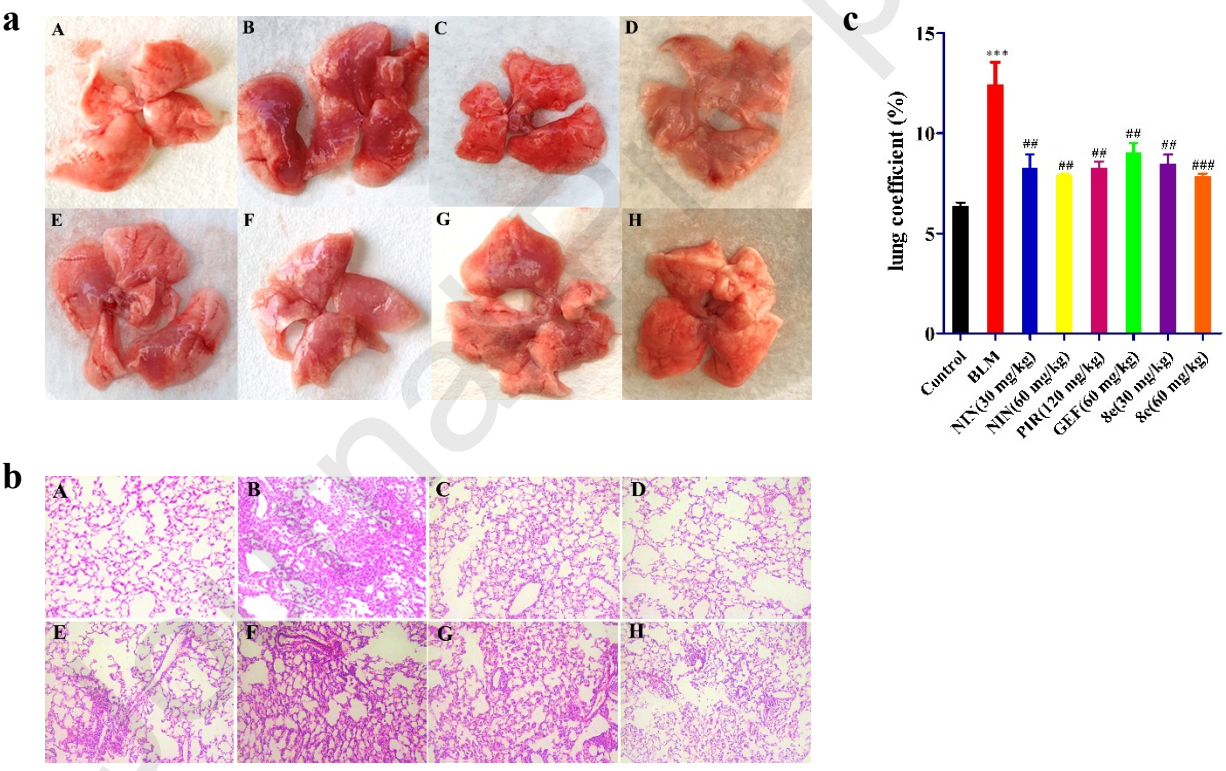

Fig. 3. The effects of **8e** and the typical anti-IPF agents on the lung morphology and lung coefficient in mouse model. The groups of C, D, E, F, G, H were given once daily for 14 days after BLM challenge (n = 8 per group). (A: The control group; B: The BLM model group; C: The BLM model plus nintedanib 30 mg/kg; D: The BLM model plus nintedanib 60 mg/kg; E: The BLM model plus pirfenidone 120 mg/kg; F: The BLM model plus gefitinib 60 mg/kg; G: The BLM model plus **8e** 30 mg/kg; H: The BLM model plus **8e** 60 mg/kg). a, The appearance of the lung; b, Representative histological lung sections stained with HE (200×); c, The lung coefficient of the mice. Data are reported as means ± SEM. ***p < 0.001 vs. the control group; ##p < 0.01 vs. the BLM group; ###p < 0.001

vs. the BLM group.

*2.2.3 **8e** reduced the collagen disposition induced by BLM in mouse lung*

Pulmonary fibrosis is characterized by excessive collagen disposition in the lung, and the content of hydroxyproline as an important marker is proportional to collagen fibers [25–27]. Masson staining results shown that BLM increased the deposition of collagen in lung, while **8e** reduced the collagen disposition induced by BLM in mouse lung (**Fig. 4a**). Accordingly, in this study, the HYP content in the mice lung tissue was determined in each mouse model group using HYP content analysis kit. The results presented in **Fig. 4b** revealed that the HYP content in the lungs of every drug-treated experimental group was significantly reduced compared with that of the untreated BLM group. These results showed that treatment with **8e** has similar biological property as nintedanib at a dose of 60 mg/kg.

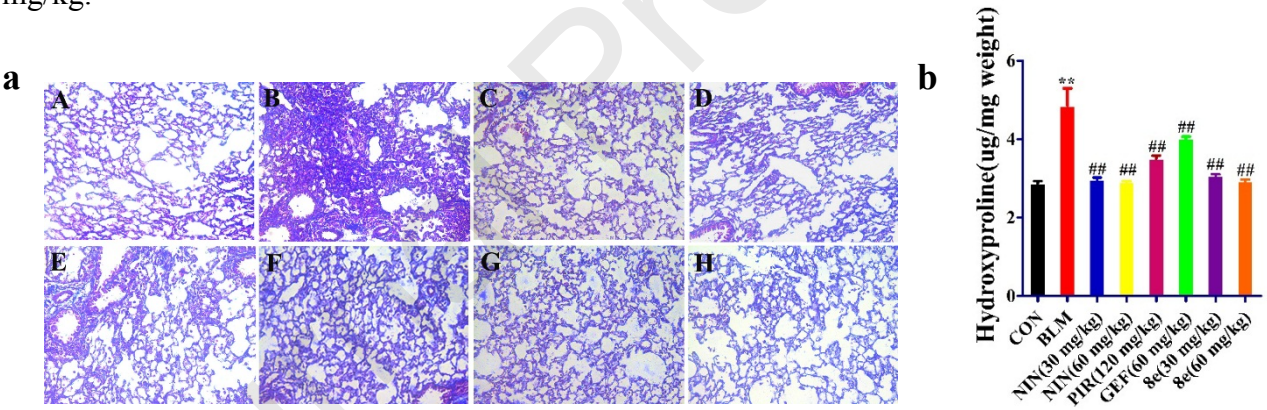

Fig. 4. The effects of **8e** and the typical anti-IPF agents on the changes of the collagen disposition in mouse model. The groups of C, D, E, F, G, H were given once daily for 14 days after BLM challenge (n = 8 per group). (A: The control group; B: The BLM model group; C: The BLM model plus nintedanib 30 mg/kg; D: The BLM model plus nintedanib 60 mg/kg; E: The BLM model plus pirfenidone 120 mg/kg; F: The BLM model plus gefitinib 60 mg/kg; G: The BLM model plus **8e** 30 mg/kg; H: The BLM model plus **8e** 60 mg/kg). a, Histological examination of Masson's Trichrome stained sections (200×); b, HYP content in model mice blood. Data are reported as means ± SEM. **p < 0.01 vs. the control group; ##p < 0.01 vs. the BLM group.

*2.2.4 **8e** attenuated BLM-induced lung inflammatory level in mice*

Malondialdehyde (MDA) is one of the most prevalent byproducts of lipid peroxidation

produced during oxidative stress [28]. Thus, we also examined the levels of this indicator. In addition, we also evaluated the effects of **8e** and the reference compounds on the expression of the inflammatory markers IL-6, IL-17A and TNF-α in the blood of BLM-induced model mice using flow cytometry analysis. As shown in **Fig. 5a–c**, **8e** clearly decreased the degree of inflammation with the increased dosage compared with the untreated control BLM model group. Moreover, treatment with **8e** attenuated the oxidant stress in the pulmonary fibrosis mice, as well as level of MDA (**Fig. 5d**). The obtained results are clearly consistent with our previous biological data described above. The levels of MDA in BLM-induced model mice treated with nintedanib or **8e** (60 mg/kg) were lower than those in the groups treated with pirfenidone (120 mg/kg) and gefitinib (60 mg/kg). Additionally, administration of **8e** also exhibited markedly enhanced effects in terms of the above-mentioned three inflammatory markers compared with the effects of pirfenidone, nintedanib, and gefitinib.

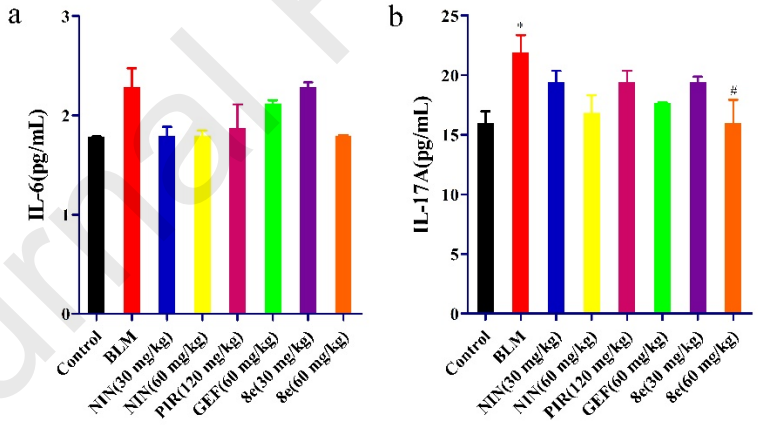

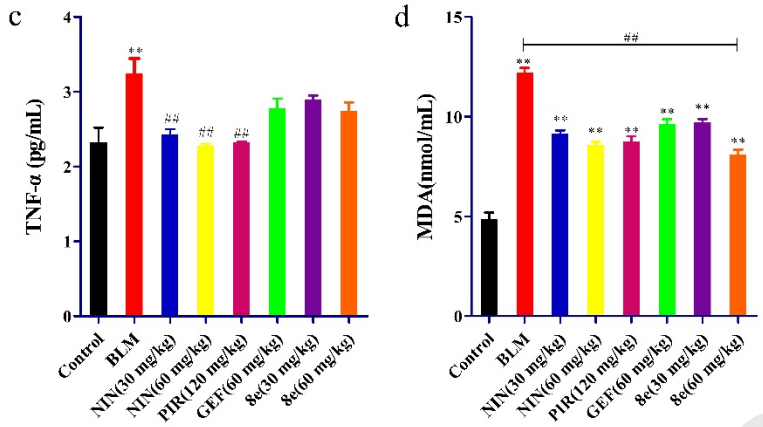

Fig. 5. The effect of **8e** and the typical anti-IPF agents on the changes of inflammatory markers in model mice blood (n = 8 per group). a, IL-6content. b, IL-17A content. c, TNF-α content. d, MDA content. Data are reported as means ± SEM. *p < 0.05 vs. the control group; #p < 0.05 vs. the BLM group; **p < 0.01 vs. the control group; ##p < 0.01 vs. the BLM group.

2.3 Molecular Simulation

Using a molecular docking simulation analysis software, three typical molecules, including the most potent JAK3 inhibitor **8e**, and two less active inhibitors, namely **8b** and **8d**, were individually docked into the binding pocket of the JAK3 protein (PDB: 4Z16) [29]. For comparison, the reference compound spebrutinib was also docked using same procedures. The simulations were performed with the Auto DOCK software version 4.2 (The Scripps Research Institute, La Jolla, CA, USA) using its default parameters [30, 31]. Among the obtained simulation conformations, only the minimal energy conformation is displayed. Additionally, the co-crystal structure of **7** with JAK3 kinase was retained for comparison.

The results shown in **Fig. 6** clearly reveal that the potent inhibitor **8e** and **7** can tightly bind with JAK3 protein in identical manner. Both compounds can form strong covalent bond between acrylamide group with amino acid Cys909. Although **8d** can also form this covalent binding, its morpholine side chain moves out of the pocket, and thus the binding contacts are reduced. When the linker between morpholine and aniline is reduced, such as **8b** or the morpholine is replaced with a

line 2-methoxyethyl substituent (spebrutinib), the type of binding with JAK3 kinase is quite different from that of **8e**. Importantly, this modification also caused the loss of the strong covalent bond. Overall, these binding models exactly explained their anti-JAK3 activity data.

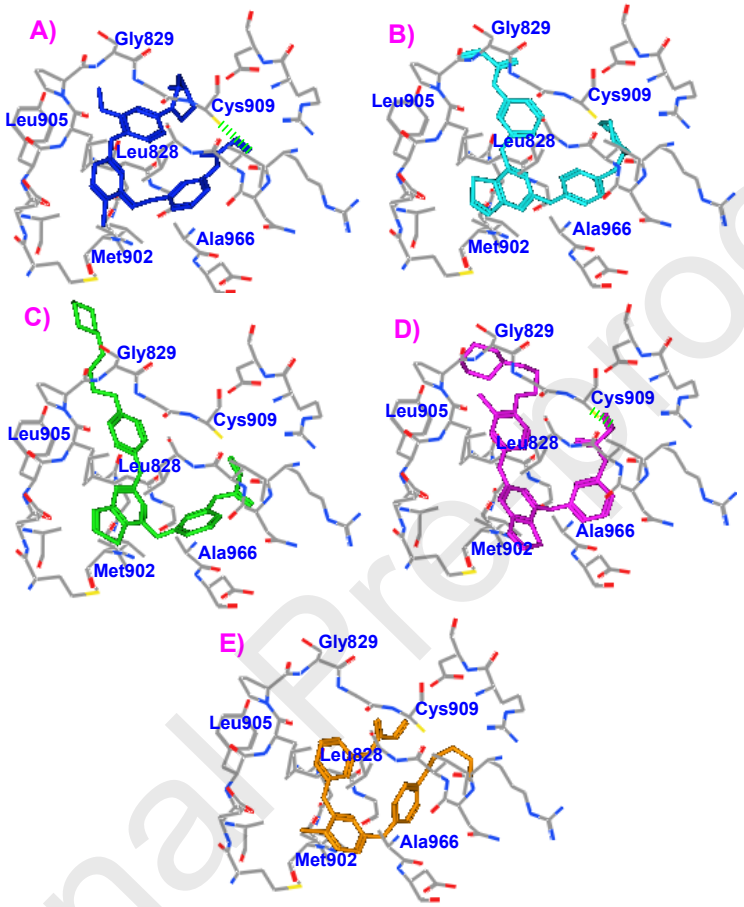

Fig. 6. Proposed binding models of the typical inhibitors with JAK3 (PDB code:4Z16). (A: **7**; B: **8b**; C: **8d**; D: **8e**; E: spebrutinib)

3. Conclusion

Selective JAK3 inhibitors play an important role in the treatment of autoimmune-related pulmonary fibrosis by regulating abnormal immune inflammatory response. This study involved the design and synthesis of a series of thieno[3,2-*d*]diphenylpyrimidines using a conformationally-constrained design strategy, and identified a potent JAK3 inhibitor, namely **8e**, which has an IC_{50} value of 1.38 nM. *In vivo* studies in the BLM-induced mouse model, after administration of **8e**,

collagen disposition and the expression of the inflammatory factor IL-6, IL-17A, TNF-α and MDA in lung tissue were reduced significantly, indicating its efficacy for the treatment of fibrosis. Overall, this work provided a new insight into the treatment of fibrosis by interfering with the JAK3 signaling pathway.

4. Experimental section

4.1 General methods for chemistry

Unless otherwise indicated, all reagents and solvents were obtained from commercial sources and used as received. 1H and 13C NMR data were obtained on a Bruker Avance at 400 and 100 MHz, respectively. Coupling constants (*J*) were expressed in hertz (Hz). Chemical shifts (δ) of NMR were reported in parts per million (ppm) units relative to internal control TMS. High-resolution ESI-MS was performed on an AB Sciex Triple TOF® 4600 LC/MS/MS system. All reactions were monitored by TLC, using silica gel plates with fluorescence F254 and UV light visualization. Flash chromatography separations were obtained on Silica Gel (300–400 mesh) using dichloromethane/methanol as eluents.

*4.2 General procedure for the synthesis of **8a-f***

A mixture of **11** (50.0 mmol), 2, 4-dichlorothieno[3,2-*d*]pyrimidine (50.0 mmol), and DIPEA (50.0 mmol) in 1,4-dioxane was gradually heated to 80 °C and stirred for 5 h. Then the mixture was diluted with water and the precipitate was filtrated to obtain crude which was purified by silica-gel column separation to get the **12a**. The similar method was carried out to the preparation of **12b**. A flask was charged with **12a-b** (0.10 mmol), **17a-f** (0.10 mmol), *p*-TsOH (0.15 mmol), and *n*-BuOH (10 mL). The slurry was heated to 70 °C for 6 h. The reaction mixture was allowed to cool to room

temperature and was neutralized with a saturated aqueous sodium bicarbonate solution. The aqueous mixture was then extracted with CH_2Cl_2 (3×20 mL). The crude product was purified using flash chromatography with dichloromethane/methanol (v/v, 30:1) as eluents.

8a *N-(3-((2-((4-(morpholinomethyl)phenyl)amino)thieno[3,2-d]pyrimidin-4-yl)amino) phenyl)acrylamide*

Yield 45.0%. off-white solid. ^{1}H NMR(DMSO-d_6): δ 10.16 (s, 1H), 9.57 (s, 1H), 9.05 (s, 1H), 8.07 (d, J = 5.3 Hz, 1H), 8.06 (s, 1H), 7.22 (d, J = 8.2 Hz, 2H), 7.56 (d, J = 7.7 Hz, 1H), 7.45 (d, J = 8.1 Hz, 1H), 7.31 (t, J = 8.0 Hz, 1H), 7.21 (d, J = 5.3 Hz, 1H), 7.10 (d, J = 8.2 Hz, 2H), 6.47 (dd, J = 16.9, 10.0 Hz, 1H), 6.27 (dd, J = 16.9, 1.4 Hz, 1H), 5.77 (dd, J = 10.0, 1.4 Hz, 1H), 3.56 (t, J = 4.3 Hz, 4H), 3.35 (s, 2H), 2.39–2.22 (m, 4H); ^{13}C NMR (DMSO-d_6): 163.6, 162.5, 158.2, 155.9, 140.6, 140.0, 139.6, 134.4, 132.4, 129.9, 129.5 (2C), 129.1, 127.3, 123.8, 118.8 (2C), 118.5, 115.2, 114.3, 108.0, 66.7 (2C), 62.7, 53.6 (2C); δ; HRMS (ESI) for $C_{26}H_{25}N_5O_3S$, $[M+H]^+$ calcd: 487.1911, found: 488.1928.

8b *N-(3-((2-((4-(morpholinomethyl)phenyl)amino)thieno[3,2-d]pyrimidin-4-yl)oxy)phenyl) acrylamide*

Yield 46.8%; off-white solid. ^{1}H NMR(DMSO-d_6): δ 10.37 (s, 1H), 9.50 (s, 1H), 8.31 (d, J = 5.3 Hz, 1H), 7.75 (t, J = 2.2 Hz, 1H), 7.63 (dd, J = 8.1, 2.2 Hz, 1H), 7.54 (d, J = 8.1 Hz, 2H), 7.47 (t, J = 8.1 Hz, 1H), 7.37 (d, J = 5.3 Hz, 1H), 7.09 (dd, J = 8.1, 2.2 Hz, 1H), 7.04 (d, J = 8.1 Hz, 2H), 6.45 (dd, J = 17.0, 10.1 Hz, 1H), 6.27 (dd, J = 17.0, 2.0 Hz, 1H), 5.79 (dd, J = 10.1, 2.0 Hz, 1H), 3.56 (t, J = 4.6 Hz, 4H), 3.35 (s, 2H), 2.31 (t, J = 4.6 Hz, 4H); ^{13}C NMR (DMSO-d_6): δ 165.2, 164.1, 163.8, 158.2, 152.7, 140.8, 139.9, 137.4, 132.1, 130.4 (2C), 129.4 (2C), 127.8, 123.7, 118.9 (2C), 117.5,

117.1, 113.4, 108.0, 66.6 (2C), 62.5, 53.5 (2C); HRMS (ESI) for $C_{26}H_{25}N_5O_3S$, $[M+H]^+$ calcd: 488.1751, found: 488.1725.

8c *N-(3-((2-((4-(2-morpholinoethoxy)phenyl)amino)thieno[3,2-d]pyrimidin-4-yl)oxy)phenyl) acrylamide*

Yield 54.2%; off-white solid. ^{1}H NMR(DMSO-d_6): δ 10.45 (s, 1H), 9.37 (s, 1H), 8.29 (d, J = 5.3 Hz, 1H), 7.73 (t, J = 2.2 Hz, 1H), 7.62 (dd, J = 8.2, 2.2 Hz, 1H), 7.55 (d, J = 8.3 Hz, 2H), 7.47 (t, J = 8.2 Hz, 1H), 7.34 (d, J = 5.3 Hz, 1H), 7.09 (dd, J = 8.2, 2.2 Hz, 1H), 6.80 (d, J = 8.3 Hz, 2H), 6.45 (dd, J = 17.0, 10.1 Hz, 1H), 6.27 (dd, J = 17.0, 2.0 Hz, 1H), 5.79 (dd, J = 10.1, 2.0 Hz, 1H), 4.25 (t, J = 5.0 Hz, 4H), 3.93–3.69 (m, 4H), 3.35–2.91 (m, 6H); ^{13}C NMR (DMSO-d_6): δ 165.2, 164.1, 163.9, 158.3, 152.7 (2C), 140.8, 137.3, 135.0, 132.1, 130.4, 127.8, 123.6, 120.7 (2C), 117.5, 117.1, 115.0 (2C), 113.4, 107.8, 64.0 (2C), 63.0, 55.8, 52.3 (2C); HRMS (ESI) for $C_{27}H_{27}N_5O_4S$, $[M+H]^+$ calcd: 518.1857, found: 518.1868.

8d *N-(3-((2-((4-(3-morpholinopropoxy)phenyl)amino)thieno[3,2-d]pyrimidin-4-yl)oxy)phenyl) acrylamide*

Yield 58.3%; off-white solid. ^{1}H NMR(DMSO-d_6): δ 10.38 (s, 1H), 9.31 (s, 1H), 8.28 (d, J = 5.3 Hz, 1H), 7.73 (t, J = 2.2 Hz, 1H), 7.62 (dd, J = 8.2, 2.2 Hz, 1H), 7.48 (d, J = 8.3 Hz, 2H), 7.47 (t, J = 8.2 Hz, 1H), 7.34 (d, J = 5.3 Hz, 1H), 7.08 (dd, J = 8.2, 2.2 Hz, 1H), 6.70 (d, J = 8.2 Hz, 2H), 6.45 (dd, J = 17.0, 10.1 Hz, 1H), 6.28 (dd, J = 17.0, 2.0 Hz, 1H), 5.79 (dd, J = 10.1, 2.0 Hz, 1H), 3.91 (t, J = 6.3 Hz, 2H), 3.58 (t, J = 4.6 Hz, 4H), 2.40 (t, J = 6.3 Hz, 2H), 2.38–2.26 (m, 4H), 1.83 (qui, J = 6.3 Hz, 2H); ^{13}C NMR (DMSO-d_6): δ 165.3, 164.1, 163.8, 158.3, 153.7, 152.7, 140.8, 137.3, 134.1, 132.1, 130.4, 127.8, 123.6, 120.7 (2C), 117.5, 117.1, 114.6 (2C), 113.4, 107.6, 66.7 (2C), 66.3, 55.4,

53.8 (2C), 26.4; HRMS (ESI) for $C_{28}H_{29}N_5O_4S$, $[M+H]^+$ calcd: 532.2013, found: 532.2019.

8e *N-(3-((2-((3-chloro-4-(3-morpholinopropoxy)phenyl)amino)thieno[3,2-d]pyrimidin-4-yl)oxy) phenyl)acrylamide*

Yield 57.2%; off-white solid. ^{1}H NMR(DMSO-d_6): δ 10.43 (s, 1H), 9.52 (s, 1H), 8.32 (d, J = 5.4 Hz, 1H), 7.80–7.62 (m, 2H), 7.61 (d, J = 8.2 Hz, 2H), 7.57–7.43 (m, 2H), 7.38 (d, J = 5.4 Hz, 1H), 7.09 (d, J = 8.2 Hz, 1H), 6.97 (d, J = 9.0 Hz, 1H), 6.46 (dd, J = 17.0, 10.1 Hz, 1H), 6.27 (dd, J = 17.0, 2.0 Hz, 1H), 5.78 (dd, J = 10.1, 2.0 Hz, 1H), 4.05 (t, J = 5.9 Hz, 2H), 3.78–3.48 (m, 4H), 3.39–2.98 m, 6H), 2.14 (qui, J = 5.9 Hz, 2H); ^{13}C NMR (DMSO-d_6): δ 165.0, 164.2, 163.8, 158.0, 152.6, 148.4, 140.9, 137.6, 135.5, 132.1, 130.5, 127.8, 123.6, 121.7, 120.4, 118.8, 117.4, 117.3, 115.0, 113.2, 108.3, 66.9, 64.0 (2C), 54.2, 51.8 (2C), 23.8; HRMS (ESI) for $C_{28}H_{28}ClN_5O_4S$, $[M+H]^+$ calcd: 566.1623, found: 566.1620.

8f *N-(3-((2-((4-((3-morpholinopropyl)thio)phenyl)amino)thieno[3,2-d]pyrimidin-4-yl)oxy) phenyl)acrylamide*

Yield 59.6%; off-white solid. ^{1}H NMR(DMSO-d_6): δ 10.39 (s, 1H), 9.59 (s, 1H), 8.32 (d, J = 5.3 Hz, 1H), 7.76 (t, J = 2.1 Hz, 1H), 7.62 (dd, J = 8.2, 2.2 Hz, 1H), 7.57 (d, J = 8.4 Hz, 2H), 7.48 (t, J = 8.2 Hz, 1H), 7.38 (d, J = 5.3 Hz, 1H), 7.12 (d, J = 8.4 Hz, 2H), 7.09 (dd, J = 8.2, 2.2 Hz, 1H), 6.45 (dd, J = 17.0, 10.1 Hz, 1H), 6.27 (dd, J = 17.0, 2.0 Hz, 1H), 5.78 (dd, J = 10.1, 2.0 Hz, 1H), 5.45 (t, J = 4.6 Hz, 4H), 2.84 (t, J = 7.1 Hz, 2H), 2.40–2.21 (m, 6H), 1.64 (qui, J = 7.1 Hz, 2H); ^{13}C NMR (DMSO-d_6): δ 165.1, 164.2, 163.8, 157.9, 152.7, 140.8, 139.7, 137.6, 132.1, 130.8 (2C), 130.5, 127.8, 127.1, 123.7, 119.6 (2C), 117.6, 117.1, 113.4, 108.2, 66.6 (2C), 57.1, 53.7 (2C), 32.2, 26.1; HRMS (ESI) for $C_{28}H_{29}N_5O_3S_2$, $[M+H]^+$ calcd: 548.1785, found: 548.1785.

4.3 Bioactivity evaluation

4.3.1 Kinase Enzymatic Assays

The ADP-Glo™ kinase assay system (JAK3: Catalog. **V3701**, Promega Corporation, USA) was used for the enzymatic biological evaluation. For the tested compounds, concentrations consisting of 0.1, 1, 10, 100, 1000 nM were used. The test was performed in a 384-well plate. All operations are carried out according to the experimental instructions, which are available at: https://cn.promega.com/products/cell-signaling/kinase-assays-and-kinase-biology/jak3-kinase-enzyme-system/?catNum=V3701). The test was performed in a 384-well plate, including the main steps below: 1) perform a 5 μL kinase reaction using 1 × kinase buffer (e.g., 1 × reaction buffer A), 2) incubate at room temperature for 60 min, 3) add 5 μL of ADP-Glo™ reagent to stop the kinase reaction and deplete the unconsumed ATP, leaving only ADP and a very low background of ATP, 4) incubate at room temperature for 40 min, 5) add 10 μL of kinase detection, 6) reagent to convert ADP to ATP and introduceluciferase and Luciferinto detect ATP, 7) incubate at room temperature for 30 min, 8) plates was measured on TriStar® LB942 Multimode MicroplateReader (BERTHOLD) to detect the luminescence (Integration time0.5–1 s). Curve fitting and data presentations were performed using GraphPad Prism version 5.0.

4.3.2 Animals

The C57BL/6J female mice weighing 20–25 g in 5–6 week–old were provided by the Laboratory Animal Center of Dalian Medical University, Dalian, China (SCXK: 2013-0003). All animals were housed in a controlled environment at 20 ± 2 °C under a 12 h dark/light cycle with free access to food and water. The animal maintenance and experiments were performed in accordance with the guidelines of the Animal Care and Use Committee.

4.3.3 Experimental Design

Mice were randomized into 8 treatment groups (n=8) were subjected to BLM-induced lung injury. Intratracheal administration of 33 μg bleomycin (Apollo Scientific) in 50 mL of sterile saline or saline alone was performed using an insulin syringe on an exposed trachea under isofluorane anesthesia. Compound **8e** was dissolved in 100% DMSO at a concentration of 100 mg/mL and aliquots stored at –20 °C. For each day, **8e** for instillation was diluted in sterile saline to give a final concentration of DMSO in the instillate of 1.4%. Three days after implantation, the mice in CON and BLM group were received by oral physiological saline (1.4% DMSO), and the mice in other six groups were oral administrated with drugs by gavage as follows: NIN (30 mg/kg) group was administrated with Nintedanib 30 mg/kg; NIN (60 mg/kg) group was administrated with Nintedanib 60 mg/kg; PIR (120 mg/kg) group was administrated with Pirfenidone 120 mg/kg; GEF (60 mg/kg) group was administrated with Gefitinib 60 mg/kg; **8e** (30 mg/kg) group was administrated with **8e** 30 mg/kg; **8e** (60 mg/kg) group was administered with **8e** 60 mg/kg. It was administered once a day for 14 days.

4.3.4 Samples

Mice were painlessly sacrificed by CO_2 inhalation and a blood sample was taken from the vena cava. The blood was added appropriate amount of 0.5% heparin sodium, followed by centrifugation with 3000 rpm for 10 min to obtain plasma. All the plasma was stored at −20 °C before test. The fresh lung was removed and weighed to calculate the lung index (lung index (%) = lung weight/body weight × 100). The entire left lobe removed for analysis of total collagen. The lungs were perfused (via the right ventricle) with 5 mL saline and the lungs lavaged with 3 × 0.8 mL phosphate buffered saline

(PBS) containing 1 mM EDTA. The lungs were removed and the entire left lobe removed for analysis of collagen. The remaining lung was inflated with 10% formalin and fixed for 24 h before embedding in paraffin wax for histological examination.

4.3.5 H&E and Massson staining

The tissue samples fixed with 4% formalin for 24 h were processed using graded alcohol, xylene and paraffin and then blocked in paraffin. The paraffin-embedded sections were sliced into 5 μm sections and stained using a hematoxylin and eosin (H&E) kit (Biyuntian, Inc., Nantong, China) and a Masson's trichrome staining kit (Nanjing Jiancheng Bioengineering Institute, Nanjing, China), according to the manufacturer's instructions. The slides with H&E staining and Masson staining were examined using light microscopy (Eclipse TE2000-S; Nikon Corporation, Tokyo, Japan) and images were captured to determine the severity of pulmonary fibrosis by a histopathologist who was blinded to the protocol design.

4.3.6 The detection of IL-6, IL-17A, TNF-α

Plasma levels of IL-6, IL-17A and TNF-α were analysed using the CBA Flex Set system (BD Biosciences) according to the manufacturer's protocol. Flow cytometry was conducted using FACSCalibur (BD Biosciences). Quantitative analysis was performed with FCAP Array v3.0 software (BD Biosciences).

4.3.7 *The detection of HYP*

The quantity of collagen in the lung tissue was determined by analysis of HYP content according to the manufacturer's instructions of the detection kit (Nanjing Jiancheng Bioengineering Institute). The absorbance was measured at 550 nm and the HYP content was determined using a formula

according to the manufacturer's instructions.

4.3.8 *The detection of MDA*

The content of malonaldehyde (MDA), a marker of oxidant stress, in mice plasma was performed using MDA kits (Biodiagnostic Company) according to the manufacturer's instructions. The absorbance was measured at 532 nm and the MDA content was determined using a formula according to the manufacturer's instructions.

4.4 Molecular docking study

The AutoDock 4.2 software was used to perform the docking exploration. Detailed tutorials that guide users through basic AutoDock usage, docking with flexible rings, and virtual screening with AutoDock may be found at: http://autodock.scripps.edu/faqs-help/tutorial. Generally, the crystal structure (PDB: 4Z16) of the kinase domain of JAK3 bound to inhibitor **8e** was used in the docking studies. The enzyme preparation and the hydrogen atoms adding was performed in the prepared process. The whole JAK3 enzyme was defined as a receptor and the site sphere was selected on the basis of the binding location of **8e**. The binding interaction energy was calculated to include Van der Waals, electrostatic, and torsional energy terms defined in the TRIPOS force field. The structure optimization was performed using a genetic algorithm, and only the best-scoring ligand protein complexes were kept for analyses.

Acknowledgments

We are grateful to the "Xing Liao" Talents Project of Liaoning province, China (XLYC1807011), the Research Fund of Higher Education of Liaoning province (LQ2017008, LQ2017039), the Natural Science Foundation of Liaoning province (20180530066), the Cultivation

Project of Youth Tech stars, Dalian, China (No. 2016RQ043), and the Foundation of Science and Technology Innovation of Dalian, China(2019J13SN76) for the financial support of this research.

Reference

[1] Raghu G, Weycker D, Edelsberg J, et al. *Am J Respir Crit Care Med*. 2006; 174: 810.

[2] Nalysnyk L, Cid-Ruzafa J, Rotella P, et al. *Eur Respir Rev*. 2012; 21: 355.

[3] Ley B, Collard HR, King TE. *Am J Respir Crit Care Med*. 2011; 183:431.

[4] Hutchinson J, Fogarty A, Hubbard R, et al. *Eur Respir J*. 2015; 46: 795.

[5] Inomata M, Kamio K, Azuma A, et al. *Respir Res*. 2014; 15:16.

[6] Xaubet A, Serrano-Mollar A, Ancochea J. *Expert Opin Pharmacother*. 2014; 15: 275.

[7] Poletti V, Ravaglia C, Tomassetti S. *Expert Rev Respir Med*. 2014; 8: 539.

[8] Horowitz JC, Thannickal VJ. *Semin Respir Crit Care Med*. 2006; 27: 600.

[9] Roth GJ, Binder R, Colbatzky F, et al. *J Med Chem*. 2015; 58:1053.

[10] Gabasa M, Ikemori R, Hilberg F, et al. *Br J Cancer*. 2017; 117:1128.

[11] Rangarajan S, Kurundkar A, Kurundkar D, et al. *Am J Respir Cell Mol Biol*. 2016; 54: 51.

[12] Richeldi L, Costabel U, Selman M, et al. *N Engl J Med*. 2011; 365: 1079.

[13] Roth GJ, Heckel A, Colbatzky F, et al. *J Med Chem*. 2009; 52: 4466.

[14] Dimitroulis IA. *Respir Care*. 2014: 59: 1450.

[15] Desroy N, Housseman C, Bock X, et al. *J Med Chem*. 2017; 60: 3580.

[16] Corless CL, Barnett CM, Heinrich MC. *Nat Rev Cancer*. 2011; 11: 71.

[17] Ishii Y, Fujimoto S, Fukuda T. *Am J Respir Crit Care Med*. 2006; 174: 550.

[18] Jamilloux Y, El Jammal T, Vuitton L, et al. *Autoimmun Rev*. 102390.

[19] Roskoski R Jr. *Pharmacol Res*. 2016; 111: 784.

[20] Thoma G, Drückes P, Zerwes HG. *Bioorg Med Chem Lett*. 2014; 24: 4617.

[21] Wrobleski ST, Pitts WJ. *Annu Rep Med Chem*. 2009; 44: 247.

[22] Ge Y, Wang CY, Song SJ, et al. *Eur J Med Chem*, 2018; 143: 1847.

[23] Song ZD, Huang SS, Yu HQ, et al. *Eur J Med Chem*. 2017; 133: 329.

[24] Szapiel SV, Elson NA, Fulmer JD, et al. *Am Rev Respir Dis*.1979; 120: 893.

[25] Ammar YA, Ismail MMF, El-Sehrawi HM, et al. *Arch Pharm*. 2006; 339: 429.

[26] Lu WQ, Yao X, Ouyang P, et al. *J Med Chem*. 2017; 60: 1817.

[27] Rajput VK, MacKinnon A, Mandal S, et al. *J Med Chem*. 2016; 59: 8141.

[28] Bartoli ML, Novelli F, Costa F, et al. *Mediators Inflamm*. 2011; 2011: 891752.

[29] Tan L, Akahane K, McNally R, et al. *J Med Chem*. 2015; 58: 6589.

[30] Wildman SA, Zheng X, Sept D, et al. *Chem Biol Drug Des*. 2011; 78: 495.

[31] Goodsell DS, Morris GM, Olson AJ. *J Mol Recognit*. 1996; 9: 1.

Graphical abstract

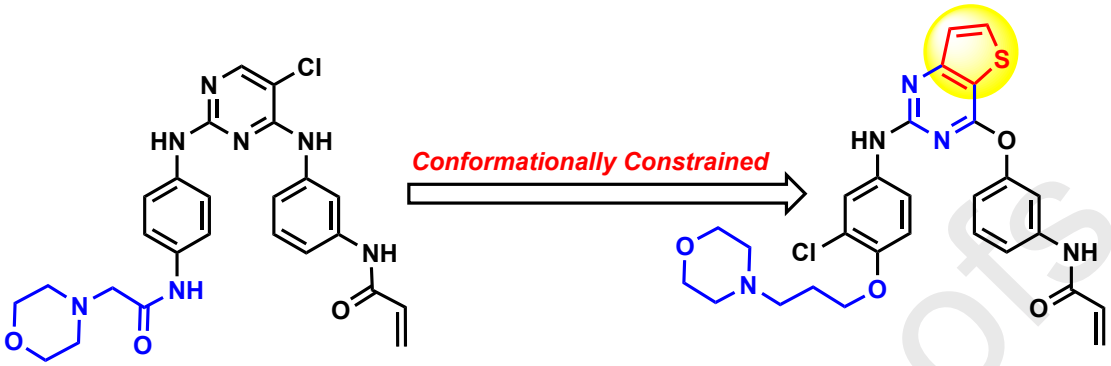

DPPY

Multi-PTK inhibitor

IC_{50}(JAK3, BTK, EGFR)<10 nM

For treatment of B-cell lymphoma

8e (Thi-DPPY)

JAK3 inhibitor(IC_{50}=1.38 nM)

BTK(IC_{50}>62.4 nM)

For treatment of IPF